

# Microsecond time-resolved X-ray scattering by utilizing MHz repetition rate at second-generation XFELs

**Sebastian Westenhoff**

`sebastian.westenhoff@kemi.uu.se`

Uppsala University

**Patrick Konold**

Laboratory of Molecular Biophysics, Institute for Cell and Molecular Biology, Uppsala University,

**Leonardo Monrroy**

Department of Chemistry - BMC, University of Uppsala <https://orcid.org/0000-0001-8852-9424>

**Alfredo Bellisario**

Laboratory of Molecular Biophysics, Institute for Cell and Molecular Biology, Uppsala University,

**Diogo Filipe**

Laboratory of Molecular Biophysics, Institute for Cell and Molecular Biology, Uppsala University,

**Patrick Adams**

RMIT University, School of Science, STEM College

**Roberto Alvarez**

Department of Physics, Arizona State University

**Richard Bean**

European X-Ray Free Electron Laser <https://orcid.org/0000-0001-8151-7439>

**Johan Bielecki**

European XFEL <https://orcid.org/0000-0002-3012-603X>

**Szabolcs Bódizs**

University of Gothenburg, Dept. of Chemistry and Molecular Biology

**Gabriel Ducroq**

Linköping University

**Helmut Grubmueller**

Max Planck Institute for Multidisciplinary Sciences

**Richard Kirian**

Arizona State University <https://orcid.org/0000-0001-7197-3086>

**Marco Kloos**

European XFEL

**Jayanat Koliyadu**

European XFEL

**Faisal Koua**

Deutsches Elektronen Synchrotron DESY, Notkestrasse 85, 22607 Hamburg, Germany.

<https://orcid.org/0000-0001-8371-9587>

**Taru Larkiala**

University of Gothenburg, Dept. of Chemistry and Molecular Biology

**Romain Letrun**

European XFEL GmbH <https://orcid.org/0000-0002-0569-5193>

**Fredrik Lindsten**

Linköping University

**Michael Maihöfer**

Max Planck Institute for Multidisciplinary Sciences

**Andrew Martin**

RMIT University <https://orcid.org/0000-0003-3704-1829>

**Petra Mészáros**

Department of Chemistry - BMC, Uppsala University

**Jennifer Mutisya**

Department of Chemistry - BMC, Uppsala University,

**Amke Nimmrich**

Department of Chemistry, University of Washington

**Kenta Okamoto**

Uppsala University <https://orcid.org/0000-0002-4858-1196>

**Adam Round**

European X-Ray Free Electron Laser <https://orcid.org/0000-0002-0723-8228>

**Tokushi Sato**

European XFEL <https://orcid.org/0000-0003-3155-3487>

**Joana Valerio**

European XFEL

**Daniel Westphal**

Uppsala University

**August Wolter**

Laboratory of Molecular Biophysics, Institute for Cell and Molecular Biology, Uppsala University

**Tej Yenupuri**

Laboratory of Molecular Biophysics, Institute for Cell and Molecular Biology, Uppsala University

**Tong You**

Laboratory of Molecular Biophysics, Institute for Cell and Molecular Biology, Uppsala University

**Filipe Maia**

Laboratory of Molecular Biophysics, Department of Cell and Molecular Biology, Uppsala University

---

## Brief Communication

**Keywords:**

**Posted Date:** December 7th, 2023

**DOI:** <https://doi.org/10.21203/rs.3.rs-3638353/v1>

**License:**  This work is licensed under a Creative Commons Attribution 4.0 International License.

[Read Full License](#)

**Additional Declarations:** There is **NO** Competing Interest.

---

**Version of Record:** A version of this preprint was published at Nature Methods on July 5th, 2024. See the published version at <https://doi.org/10.1038/s41592-024-02344-0>.

## Microsecond time-resolved X-ray scattering by utilizing MHz repetition rate at second-generation XFELs

Patrick E. Konold\*<sup>1</sup>, Leonardo Monrroy\*<sup>2</sup>, Alfredo Bellisario<sup>1</sup>, Diogo Filipe<sup>1</sup>, Patrick Adams<sup>4</sup>, Roberto Alvarez<sup>5</sup>, Richard Bean<sup>6</sup>, Johan Bielecki<sup>6</sup>, Szabolcs Bódizs<sup>3</sup>, Gabriel Ducrocq<sup>9,10</sup>, Helmut Grubmueller<sup>7</sup>, Richard A. Kirian<sup>5</sup>, Marco Kloos<sup>6</sup>, Jayanath C. P. Koliyadu<sup>6</sup>, Faisal H. M. Koua<sup>6</sup>, Taru Larkiala<sup>3</sup>, Romain Letrun<sup>6</sup>, Fredrik Lindsten<sup>9,10</sup>, Michael Maihöfer<sup>7</sup>, Andrew V. Martin<sup>4</sup>, Petra Mészáros<sup>2</sup>, Jennifer Mutisya<sup>2</sup>, Amke Nimmrich<sup>3,8</sup>, Kenta Okamoto<sup>1</sup>, Adam Round<sup>6</sup>, Tokushi Sato<sup>6</sup>, Joana Valerio<sup>6</sup>, Daniel Westphal<sup>1</sup>, August Wollter<sup>1</sup>, Tej Varma Yenupuri<sup>1</sup>, Tong You<sup>1</sup>, Filipe Maia<sup>+1</sup>, Sebastian Westenhoff<sup>+2,3</sup>

\* equal contribution

+ Corresponding [filipe.maia@icm.uu.se](mailto:filipe.maia@icm.uu.se), [sebastian.westenhoff@kemi.uu.se](mailto:sebastian.westenhoff@kemi.uu.se)

<sup>1</sup>Laboratory of Molecular Biophysics, Institute for Cell and Molecular Biology, Uppsala University, Box 596, 75124 Uppsala, Sweden

<sup>2</sup>Department of Chemistry - BMC, Uppsala University, Box 576, 75123, Uppsala, Sweden

<sup>3</sup>Department of Chemistry and Molecular Biology, University of Gothenburg, Gothenburg, Sweden

<sup>4</sup>School of Science, STEM College, RMIT University, Melbourne, Victoria 3000, Australia

<sup>5</sup>Department of Physics, Arizona State University, 550 E. Tyler Dr., Tempe, AZ, 85287, USA

<sup>6</sup>European XFEL, Holzkoppel 4, 22869, Schenefeld, Germany

<sup>7</sup>Max Planck Institute for Multidisciplinary Sciences, Am Fassberg 11, 37077 Göttingen, Germany

<sup>8</sup>Department of Chemistry, University of Washington, Bagley Hall, Seattle, WA 98195, USA

<sup>9</sup>Department of Computer and Information Science (IDA), Linköping University, 58183, Linköping, Sweden

<sup>10</sup>The Division of Statistics and Machine Learning (STIMA), Linköping University, 58183, Linköping, Sweden



## Abstract

Detecting microsecond structural perturbations in biomolecules has wide relevance in biology, chemistry, and medicine. Here, we show how MHz repetition rates at X-ray free electron lasers (XFELs) can be used to produce microsecond time-series of protein scattering with exceptionally low noise levels of 0.001%. We demonstrate the approach by deriving new mechanistic insight into  $\alpha$  helix unfolding of a Light-Oxygen-Voltage (LOV) photosensory domain. This time-resolved acquisition strategy is easy to implement and widely applicable for direct observation of structural dynamics of many biochemical processes.

## Main Text

Biomolecular transformations, reactions, and interactions are at the basis of all life. Deciphering these mechanisms in a time-resolved manner and with sub-molecular precision opens a new dimension of biological understanding. Access to sub-millisecond timescales in near-native environments is particularly important, but remains challenging.

There are two primary acquisition schemes to acquire time-resolved data. In 'pump-probe' mode, each reaction trigger is followed by a probe pulse at a defined time delay and time-series are constructed by repeated measurement of many time points. This mode enables femtosecond time-resolution and has been used at XFELs for time-resolved protein crystallography and protein solution scattering<sup>1-3</sup>. In practice, this method limits acquisition rates leading to larger sample consumption. An alternative approach is to read out a series of probe pulses following a single trigger event. In this way, the efficiency of data collection is vastly improved, reducing sample consumption and suppressing experimental noise through massive averaging<sup>4</sup>. Here, the time-resolution is limited by the X-ray repetition and detector acquisition rates.

MHz repetition rates at second-generation XFELs now open up the opportunity to use the latter scheme for time-resolved studies in the microsecond range. The European XFEL (EuXFEL) is the first in this class and delivers trains at 10 Hz containing up to 2700 X-ray pulses with a variable repetition rate up to 4.5 MHz (Figure 1b)<sup>5</sup>. Thus far, the high repetition rate has posed severe technical challenges for single-pulse detection of scattering and diffraction images, due to electronic noise and nonlinear gain in the detector readout, as well as shockwaves or explosions in the jet<sup>6</sup>. For these reasons, this unique timing capability has only been used in X-ray microscopy, dynamic compression experiments, and X-ray photon correlation spectroscopy,<sup>7-9</sup> but not yet in the pursuit of biomolecular structural dynamics

through protein scattering. Here, we demonstrate the realization of this approach through time-resolved wide-angle X-ray scattering (TR-WAXS) at the EuXFEL.

TR-WAXS can resolve structural changes of biomolecules and chemicals in solution, providing an ~atomic-scale glimpse of their function under near-native conditions<sup>4,10,11</sup>. We investigate the phototropin LOV2 domain from *Avena sativa* (AsLOV2), which features a prototypical signaling mechanism, where a C-terminal helix (J $\alpha$ , 22 residues) detaches from the core in response to photoexcitation<sup>12,13</sup>. This unique photoactivity has been exploited in a broad range of optogenetic applications and has been the subject of intense experimental investigation<sup>14–19</sup>. Despite this interest, the mechanism and timing of J $\alpha$  unfolding and the structure of the unfolded state are not definitively known.

To record microsecond TR-WAXS at the EuXFEL, the sample was carried in a liquid jet via 3D-printed Gas Dynamic Virtual Nozzle (GDVN)<sup>20</sup> to the interaction point of the optical and X-ray beams at the Single Particles, Clusters, and Biomolecules and Serial Femtosecond Crystallography (SPB/SFX) endstation (Figure 1a)<sup>21</sup>. Photoexcitation was achieved with nanosecond laser pulses timed to the start of every second X-ray pulse train (Figure 1b). The scattering was recorded on the AGIPD detector for each probe pulse, covering a  $q$ -range from  $2.1 \text{ \AA}^{-1} > q > 0.08 \text{ \AA}^{-1}$  (corner resolution). The 2D scattering was integrated into rings as a function of the momentum transfer ( $q$ ) and delay time ( $t$ ) along the pulse train. Approximately 30% of the data were excluded, because the shape of the scattering was affected by fluctuations in the jet (see online methods). After averaging over several repeats, the difference scattering  $\Delta S = S_{light}(q,t) - S_{dark}(q,t)$  was computed (Figure 1c). We found that it was crucial to subtract entire laser-on from the laser-off trains from each other, reducing the effect of systematic noise in the detector (Supplementary Figure 2). An experimental time resolution of  $1.77 \text{ \mu s}$  corresponds to the inverse of the repetition rate of the XFEL (564 kHz) and the data span a time window of  $\sim 300 \text{ \mu s}$ .

The X-ray scattering of AsLOV2 shows microsecond evolution with oscillations extending beyond  $q$ -values of  $1.5 \text{ \AA}^{-1}$ , which translates into a spatial resolution of  $4.2 \text{ \AA}$ . The data have an exceptionally low noise floor corresponding to 0.001% of the total signal, which is at least one order of magnitude lower than previous accounts for this method (Supplementary Figure 3)<sup>22</sup>. Deconvolution of the data using spectral decomposition with exponential conversion laws indicated that the data are best fit to a sequential model of type  $A \rightarrow B \rightarrow C$ , yielding base patterns for the three states (Figure 2b, Supplementary Figure 4). In TR-WAXS, large difference signals at low  $q < 0.15 \text{ \AA}^{-1}$  typically indicate changes of the radius of gyration ( $R_g$ ) of the protein<sup>3</sup>. From this we deduce that the structural change in state C is sizable, but that

changes in states A and B are comparably smaller. We assign state C to the unfolded state (*vide infra*), which is further underpinned by its timescale, emerging within  $\sim 300 \mu\text{s}$  (Figure 2a), in agreement with kinetics inferred from infrared spectroscopy<sup>17,18</sup>. States A and B could only be resolved because of the low noise floor of the new scattering method approach. State A forms within the first time point of our measurement at  $1.77 \mu\text{s}$ , in agreement with previous reports of FMN-cysteinyI adduct formation<sup>23</sup>. We assign state B to a previously unrecognized intermediate state, which occurs subsequent to Cys adduct formation and prior to large changes in the J $\alpha$  helix. Interestingly, intermediate states in J $\alpha$  unfolding have been previously proposed through a long MD simulation<sup>24</sup>, but not clearly observed experimentally.

Focusing on state C and to assess the extent of J $\alpha$  unfolding, we refined structural models predicted by AlphaFold<sup>25</sup>, where a large variability was obtained through sampling with dropout enabled inference (20000 structures predicted)<sup>26</sup> and a number of glycine mutations in the J $\alpha$  helix. We then determined best fits against the predicted structures by comparison of the root-mean-square of residuals ( $R^2$ ) between theoretical and experimental difference scattering curves (Figure 2d). Since we compare the curves on absolute scales, this selection is also based on appropriate computed activation factors of the structural pairs (further described in Supplementary Information, the boxed region in Figure 2c includes 6032 structures). All of the selected structures show unfolded J $\alpha$  helices (subset shown in Figure 2f), with an increase of R $g$  by 5-7Å yielding the best fits (Figure 2e). Interestingly, an inspection of the best-fitting models shows that the residues directly preceding the J $\alpha$  segment, which form a loop segment in the dark, form an ordered helical domain (Supplementary Figure 7). Finally, we find that the N-terminal A' $\alpha$  helix is unfolded in most structures. Our data establishes that (i) the J $\alpha$  helix unfolds in a two-step mechanism within  $300 \mu\text{s}$ , (ii) that it completely unfolds, and (iii) that additional structural changes accompany this process. This concludes a long series of investigations into J $\alpha$  unfolding<sup>14-19,24</sup>, and demonstrates the promising capability of this new time-resolved X-ray scattering method.

Our new implementation of TR-WAXS realizes the unused potential of MHz XFELs to provide unique structural information about transient states on the important microsecond timescale. The additional timing information is gained with only minor adjustments of existing XFEL acquisition schemes and is highly compatible with other methods that use short X-ray pulses, e.g. serial crystallography<sup>1-3</sup> or X-ray emission spectroscopy<sup>27</sup>. The method also exploits the high average X-ray flux at the EuXFEL resulting in exceptionally low noise levels. This enabled the identification of a new transient state in J $\alpha$  unfolding, opening the door for investigating reaction dynamics with dilute samples of proteins, peptides, RNA or



DNA, especially when combined with ongoing development of ultrastable liquid jet sample injection technology<sup>28</sup>. It also permits detection of difference scattering signals to very high scattering angles ( $q > 1.5 \text{ \AA}^{-1}$ , Figure 1c), suggesting that time-resolved and high-resolution structural information can be obtained in crystallography<sup>29-31</sup> or single-particle diffraction experiments<sup>32</sup>. Overall, the presented method accelerates knowledge gain for dynamic enzymatic and chemical mechanisms.

## Figures

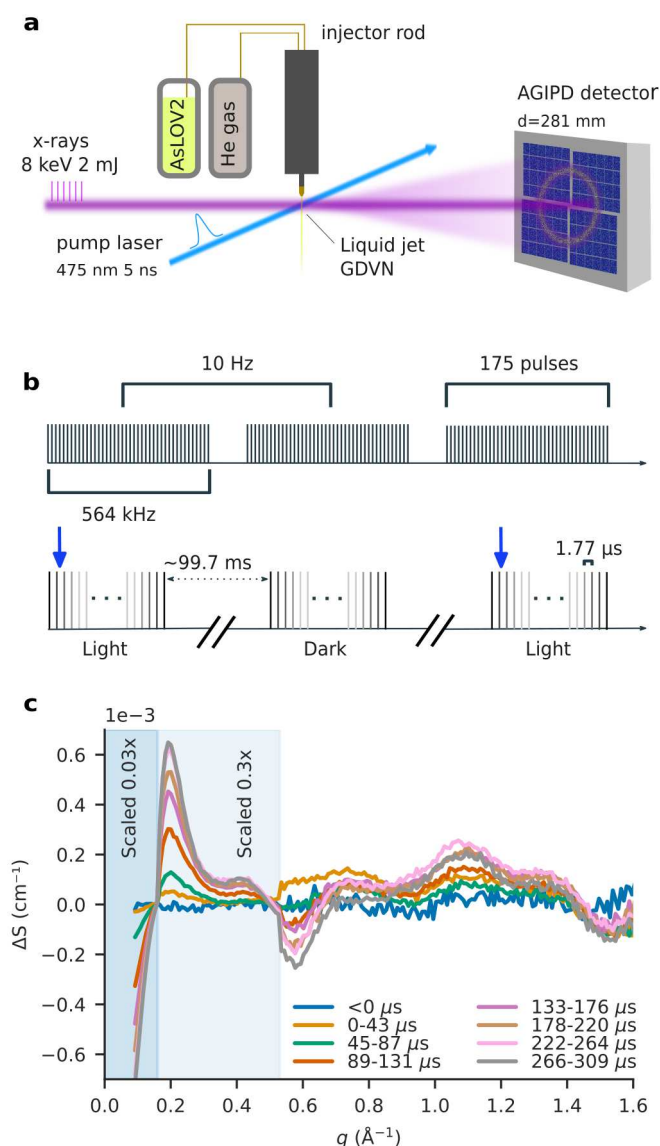


**Figure 1. Microsecond TR-WAXS facilitating the MHz repetition rate at the EuXFEL. a.** Schematic depiction of the X-ray and optical laser path, GDVN liquid jet, and recorded scattering with the AGIPD detector (not drawn to scale). **b.** Pulse train structure and laser excitation scheme used to obtain microsecond time-resolution. The 10 Hz trains comprise 175 pulses at 564 kHz (1.77  $\mu$ s interval). The blue arrow depicts the timing of optical excitation of every other pulse train. **c.** TR-WAXS data of AsLOV2. The momentum transfer was defined as  $q = 4\pi \sin \theta / \lambda$ , with  $2\theta$  and  $\lambda$  as the scattering angle and the X-ray wavelength, respectively. The data was normalized in the  $q$ -range  $1.6 \text{ \AA}^{-1} > q > 1.4 \text{ \AA}^{-1}$ , and scaled for better visualization as indicated in the panel.

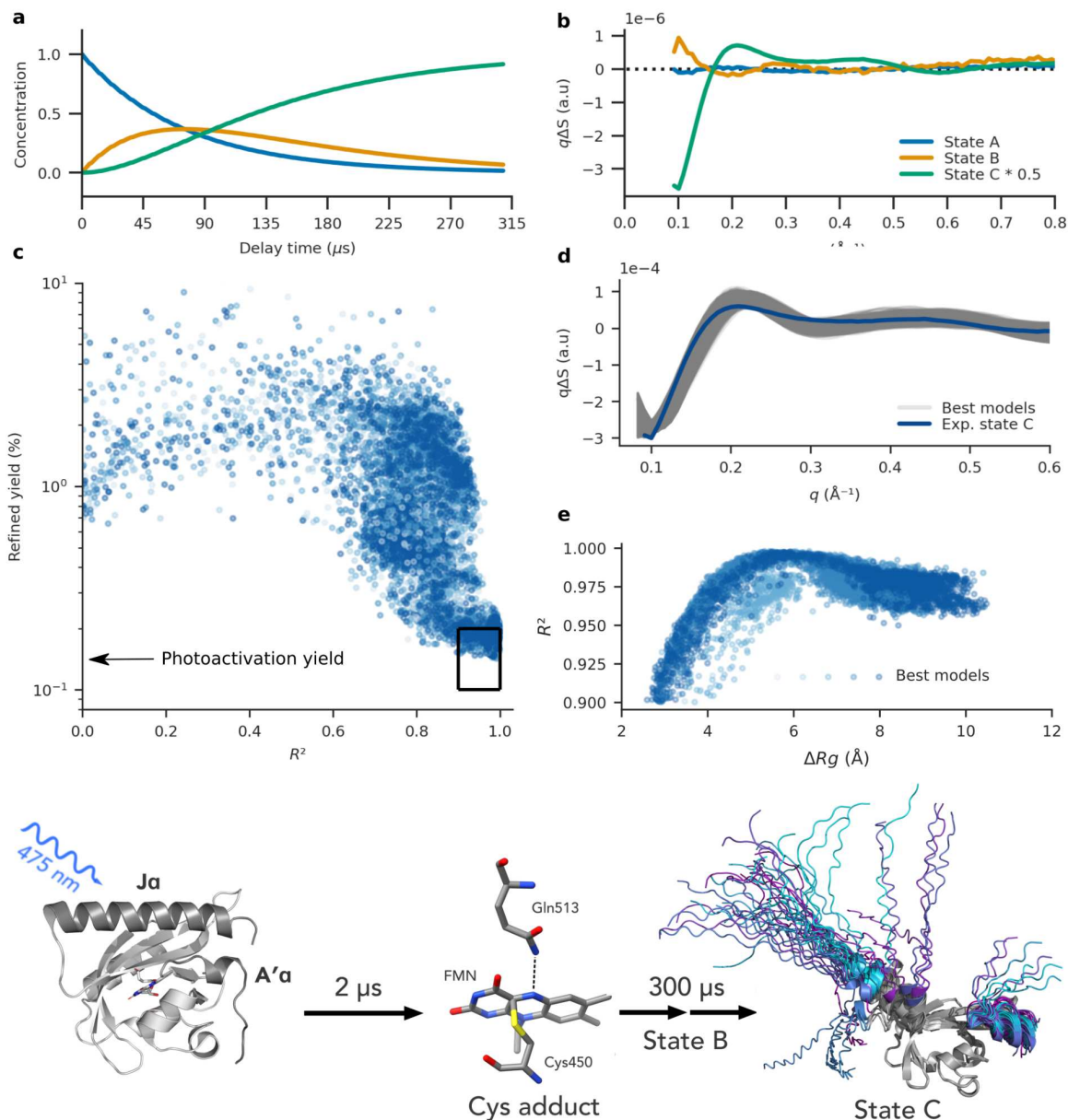


**Figure 2. TR-WAXS yields a new intermediate state and the structure of the Ja unfolded state in a LOV domain protein.**

**a.** The time evolution of constituent states and **b.** their spectral components derived from kinetic decomposition of TR-WAXS data. **c.** Structural modeling results generated using our adapted AlphaFold method.  $R^2$  is used as an indicator of a good fit between experimental and theoretical difference signals. Darker blue shades correspond to increasing numbers of mutations in the Ja helix. Structures with mutations in the N-terminal helix are also included. The best models were selected by choosing those that have both a photoactivation yield of  $15 \pm 5\%$  (as derived in supplementary Figure 6) and  $R^2 > 0.9$ , resulting in 6032 candidate models (black box). **d.** The theoretical difference scattering of the best fits (gray) and the scaled experimental scattering profile of state C (blue) are shown. **e.**  $R^2$  of the top candidate structures versus change in radius of gyration ( $\Delta Rg$ ). **f.** The new structural dynamics results are shown in the canonical photoactivation mechanism of AsLOV2. This work finds that Ja unfolding occurs in a biphasic manner

within 300  $\mu$ s. The structure of the unfolded state C is depicted as a subset of 50 selected from the best fits.

## Acknowledgements

S.W., F.M., and H.G. acknowledge support by the Swedish Research Council and the BMBF for this research. The sample reservoirs employed in parts of the measurements presented here were designed and fabricated by the Max Planck Institute for Medical Research, Heidelberg, which also provided instruction in its use. P.A. and A.V.M. acknowledge the support of the Universities Australia and the German Academic Exchange Service (DAAD) for this research. We thank Kevin Gardner at CUNY for sharing the AsLOV2 plasmid. We acknowledge the use of the European XFEL biological sample preparation laboratory, enabled by the XBI User Consortium. We acknowledge European XFEL in Schenefeld, Germany, for provision of X-ray free-electron laser beamtime at Scientific Instrument SPB/SFX and would like to thank the SPB/SFX instrument group and facility staff for their assistance. J.V. acknowledges funding from the European Union's Horizon 2020 research and innovation program under grant agreement no. 101004728. R.K. acknowledges funding from the National Science Foundation, BioXFEL Science and Technology Center (award #1231306) and Directorate for Biological Sciences (award #1943448). Alpha Fold computations were enabled by resources provided by the National Academic Infrastructure for Supercomputing in Sweden (NAISS) at NSC Berzelius partially funded by the Swedish Research Council through grant agreement no. 2022-06725

## Data availability

The raw experimental data is available at the EuXFEL repository: <https://doi.org/10.22003/XFEL.EU-DATA-003046-00>. The refined protein structures are also provided within this database.

## REFERENCES

1. Pandey, S. *et al.* Time-resolved serial femtosecond crystallography at the European XFEL. *Nat. Methods* **17**, 73–78 (2020).
2. Barends, T. R. M. *et al.* Direct observation of ultrafast collective motions in CO myoglobin upon ligand dissociation. *Science* **350**, 445–450 (2015).
3. Levantino, M. *et al.* Ultrafast myoglobin structural dynamics observed with an X-ray free-electron laser. *Nat. Commun.* **6**, 6772 (2015).
4. Westenhoff, S. *et al.* Rapid readout detector captures protein time-resolved WAXS. *Nat. Methods* **7**, 775–776 (2010).
5. Decking, W. *et al.* Author Correction: A MHz-repetition-rate hard X-ray free-electron laser driven by a superconducting linear accelerator. *Nat. Photonics* **14**, 650–650 (2020).
6. Grünbein, M. L. *et al.* Effect of X-ray free-electron laser-induced shockwaves on haemoglobin microcrystals delivered in a liquid jet. *Nat. Commun.* **12**, 1672 (2021).
7. Vagovič, P. *et al.* Megahertz x-ray microscopy at x-ray free-electron laser and synchrotron sources. *Optica* **6**, 1106 (2019).
8. Dallari, F. *et al.* Microsecond hydrodynamic interactions in dense colloidal dispersions probed at the European XFEL. *IUCrJ* **8**, 775–783 (2021).

9. Husband, R. J. *et al.* A MHz X-ray diffraction set-up for dynamic compression experiments in the diamond anvil cell. *J. Synchrotron Radiat.* **30**, 671–685 (2023).
10. Cammarata, M. *et al.* Tracking the structural dynamics of proteins in solution using time-resolved wide-angle X-ray scattering. *Nat. Methods* **5**, 881–886 (2008).
11. Ki, H., Oang, K. Y., Kim, J. & Ihee, H. Ultrafast X-Ray Crystallography and Liquidography. *Annu. Rev. Phys. Chem.* **68**, 473–497 (2017).
12. Harper, S. M., Neil, L. C. & Gardner, K. H. Structural basis of a phototropin light switch. *Science* **301**, 1541–1544 (2003).
13. Harper, S. M., Neil, L. C., Day, I. J., Hore, P. J. & Gardner, K. H. Conformational changes in a photosensory LOV domain monitored by time-resolved NMR spectroscopy. *J. Am. Chem. Soc.* **126**, 3390–3391 (2004).
14. Chen, E., Swartz, T. E., Bogomolni, R. A. & Kliger, D. S. A LOV story: the signaling state of the phot1 LOV2 photocycle involves chromophore-triggered protein structure relaxation, as probed by far-UV time-resolved optical rotatory dispersion spectroscopy. *Biochemistry* **46**, 4619–4624 (2007).
15. Nakasone, Y., Eitoku, T., Matsuoka, D., Tokutomi, S. & Terazima, M. Dynamics of conformational changes of Arabidopsis phototropin 1 LOV2 with the linker domain. *J. Mol. Biol.* **367**, 432–442 (2007).
16. Eitoku, T., Nakasone, Y., Matsuoka, D., Tokutomi, S. & Terazima, M. Conformational dynamics of phototropin 2 LOV2 domain with the linker upon photoexcitation. *J. Am. Chem. Soc.* **127**, 13238–13244 (2005).
17. Konold, P. E. *et al.* Unfolding of the C-Terminal J $\alpha$  Helix in the LOV2 Photoreceptor Domain Observed by Time-Resolved Vibrational Spectroscopy. *J. Phys. Chem. Lett.* **7**, 3472–3476 (2016).
18. Gil, A. A. *et al.* Femtosecond to Millisecond Dynamics of Light Induced Allostery in the Avena sativa LOV Domain. *J. Phys. Chem. B* **121**, 1010–1019 (2017).
19. Yao, X., Rosen, M. K. & Gardner, K. H. Estimation of the available free energy in a LOV2-J  $\alpha$  photoswitch. *Nat. Chem. Biol.* **4**, 491–497 (2008).
20. DePonte, D. P. *et al.* Gas dynamic virtual nozzle for generation of microscopic droplet streams. *J. Phys. D Appl. Phys.* **41**, 195505 (2008).
21. Mancuso, A. P. *et al.* The Single Particles, Clusters and Biomolecules and Serial Femtosecond Crystallography instrument of the European XFEL: initial installation. *J. Synchrotron Radiat.* **26**, 660–676 (2019).
22. Berntsson, O. *et al.* Sequential conformational transitions and  $\alpha$ -helical supercoiling regulate a sensor histidine kinase. *Nat. Commun.* **8**, 284 (2017).
23. Kennis, J. T. M. *et al.* Primary reactions of the LOV2 domain of phototropin, a plant blue-light photoreceptor. *Biochemistry* **42**, 3385–3392 (2003).
24. Iuliano, J. N. *et al.* Unraveling the mechanism of a LOV domain optogenetic sensor: A glutamine lever induces unfolding of the j $\alpha$  helix. *ACS Chem. Biol.* **15**, 2752–2765 (2020).
25. Jumper, J. *et al.* Highly accurate protein structure prediction with AlphaFold. *Nature* **596**, 583–589 (2021).
26. Wallner, B. AFsample: Improving Multimer Prediction with AlphaFold using Aggressive Sampling. *BioRxiv* (2022) doi:10.1101/2022.12.20.521205.
27. Kern, J. *et al.* Structures of the intermediates of Kok's photosynthetic water oxidation clock. *Nature* **563**, 421–425 (2018).
28. Konold, P. E. *et al.* 3D-printed sheet jet for stable megahertz liquid sample delivery at X-ray free-electron lasers. *IUCrJ* (2023) doi:10.1107/S2052252523007972.
29. Chapman, H. N. *et al.* Femtosecond X-ray protein nanocrystallography. *Nature* **470**, 73–77 (2011).
30. Grünbein, M. L. *et al.* Megahertz data collection from protein microcrystals at an X-ray free-electron laser. *Nat. Commun.* **9**, 3487 (2018).
31. Wiedorn, M. O. *et al.* Megahertz serial crystallography. *Nat. Commun.* **9**, 4025 (2018).
32. Sobolev, E. *et al.* Megahertz single-particle imaging at the European XFEL. *Commun. Phys.* **3**, 97 (2020).

## Supplementary Files

This is a list of supplementary files associated with this preprint. Click to download.

- [briefAsLOV2TRWAXSSupportingInformation1.pdf](#)
- [allstructuresubmission.zip](#)